Enhanced PSpice Model of TiO2 Memristor

Zdenek Kolka, Dalibor Biolek, Viera Biolkova

Abstract—The present paper enhances Pickett's model of the TiO$_2$ memristor by modifying its Port Equation in order to eliminate a non-physical negative resistance region that occurs at higher currents. This region causes an ambiguity of the static I-V characteristic, which may bring non-convergence, numerical errors, and non-physical solutions during time-domain simulation. The modification is based on the tangential extrapolation. Full listing of the (P)Spice macromodel is provided.

Keywords—TiO2 memristor, Port Equation, State Equation, Pickett's model, Spice, simulation.

I. INTRODUCTION

MEMRISTORS are considered the key components for future memory, logic, and neuromorphic systems [1], [2]. Although the resistive switching phenomenon has been known for a long time, the recognizing memristor in the TiO$_2$ device manufactured by HP labs in 2008 has brought feverish interest in this area [3], [4].

A two-terminal mem-system of the *n*-th order is defined by the following equations [4]

Port Equation (PE): $y(t) = g(\mathbf{x}, u, t) u(t)$, $\qquad$ (1)

State Equation (SE): $\dot{\mathbf{x}} = f(\mathbf{x}, u, t)$ $\qquad$ (2)

where $u(t)$ and $y(t)$ represent voltage (v), current (i) or derived quantities like charge (q) and flux (φ); $u(t)$ is the controlling quantity, $y(t)$ is the dependent quantity, and the function g is the generalized response. In the case of memristive systems, (1) relates voltage and current [5]. The internal state of the mem-system is represented by the *n*-dimensional state vector $\mathbf{x}$, whose evolution is governed by the vector field f. Using formalisms (1) and (2), the problem of modeling a memristive system is divided into the modeling of static I-V characteristics (PE) and the modeling of switching dynamics (SE).

A hot topic of current mem-system research is to formulate

Z. Kolka is with the Department of Radio Electronics, Brno University of Technology, Technicka 12, 616 00 Brno, Czech Republic (phone: +420-541146554; e-mail: kolka@feec.vutbr.cz).

D. Biolek is with the Department of Electrical Engineering, University of Defence, Kounicova 65, 662 10 Brno, Czech Republic (e-mail: dalibor.biolek@unob.cz).

V. Biolkova is with the Department of Radio Electronics, Brno University of Technology, Technicka 12, 616 00 Brno, Czech Republic (e-mail: biolkova@feec.vutbr.cz).

sufficiently accurate yet simple models for physical devices. The first group of well-known models was based on the concept of linear SE introduced in [3], where the state variable is unbounded. To keep the state variable within physical bounds, the model was later completed with the so-called window functions by Joglekar [6], Biolek [7], Prodromakis [8] and others. These models are popular for their simplicity, easy implementation in SPICE and the possibility of obtaining an analytical solution but, as shown in a comprehensive study [9], they are not able to capture the complex nonlinear behavior of real devices.

The only physical model of the TiO$_2$ memristor published so far is Pickett's model [10], whose SPICE implementation was provided in [11]. The model represents very well both the static characteristics and the switching dynamics but its simulation has been found sensitive to changes of the excitation signal [9], [12]. It can be shown that the solution of the Port Equation of Pickett's model is ambiguous, which seems to be the origin of non-convergence, numerical errors, and non-physical solutions obtained during time-domain simulations.

The purpose of the present paper is to propose a modification of Pickett's model based on the use of tangential extrapolation and to implement the modification in a PSpice simulation model. Section II of the paper presents the analysis and extrapolation of the model, and Section III demonstrates its properties in comparison with the original model.

II. PHYSICAL MODEL OF TiO$_2$ MEMRISTOR

A. Original Pickett's model

The HP memristor is composed of a thin TiO$_2$ layer between two platinum electrodes. After an electroforming process, most of the oxide is transformed into a highly conductive channel with oxygen vacancies except for a nanometer insulating barrier near the positive electrode, which forms a tunneling barrier. The barrier width and thus the memristor characteristics can be influenced reversibly by a voltage applied across the memristor [10].
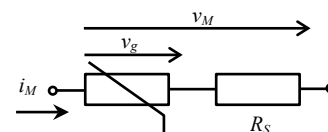

Fig. 1. Equivalent schematics of the Port Equation in Pickett's model [10].

The only physical model of the HP memristor published so far is Pickett's model [10], [11]. The Port Equation (1) is represented in an implicit form by a series connection of a

resistor R_S and a nonlinear Metal-Insulator-Metal (MIM) tunneling junction, Fig. 1.

The tunneling current is expressed by Simmons's formula for MIM junctions with image forces [13] as a function of the internal voltage v_g and the barrier width w, which was chosen as the state variable. The equations read

$$i_M = \frac{\text{sgn}(v_g)j}{\Delta w^2}\left\{\phi_I \exp\left(-B\Delta w\sqrt{\phi_I}\right)- \right.$$
$$\left. -\left(\phi_I + e|v_g|\right)\exp\left(-B\Delta w\sqrt{\phi_I + e|v_g|}\right)\right\} \quad (3)$$

where

$$j = \frac{Ae}{2\pi\hbar}, \quad B = \frac{4\pi\sqrt{2m}}{\hbar}, \quad \lambda = \frac{e^2\ln(2)}{8\pi\varepsilon_r\varepsilon_0 w}, \quad (4a,b,c)$$

$$w_1 = \frac{1.2\lambda w}{\phi_0}, \quad w_2 = w_1 + w\left(1 - \frac{9.2\lambda}{3\phi_0 + 4\lambda - 2e|v_g|}\right), \quad (5a,b)$$

$$\Delta w = w_2 - w_1, \quad (6)$$

$$\phi_I = \phi_0 - e|v_g|\frac{w_1 + w_2}{2w} - \frac{1.15\lambda w}{\Delta w}\ln\left[\frac{w_2(w - w_1)}{w_1(w - w_2)}\right]. \quad (7)$$

The symbol A represents the junction area, e is the electron charge, m is the electron mass, $\hbar$ is the Planck constant, ε_r is the dielectric constant of the insulator, and ϕ_0 is the barrier height. The variables w_1 and w_2 represent the barrier limits at the Fermi level, and ϕ_I is the mean barrier height. The model is symmetric with respect to the applied voltage v_g.

The state equation reflects the highly asymmetric dynamical behavior of the TiO$_2$ memristor for ON switching ($i_M < 0$) and OFF switching ($i_M > 0$) [10]

$$\frac{dw}{dt} = \begin{cases} f_{off}\sinh\left(\dfrac{i_M}{i_{off}}\right)\exp\left(-\exp\left(\dfrac{w - a_{off}}{w_c} - \dfrac{|i_M|}{b}\right) - \dfrac{w}{w_c}\right) & \text{for } i_M \geq 0 \\[3ex] f_{on}\sinh\left(\dfrac{i_M}{i_{on}}\right)\exp\left(-\exp\left(\dfrac{a_{on} - w}{w_c} - \dfrac{|i_M|}{b}\right) - \dfrac{w}{w_c}\right) & \text{for } i_M < 0 \end{cases}. \quad (8)$$

All parameters in (8) are mere fitting parameters without any direct physical meaning.

Paper [10] presents the parameters of Pickett's model identified for a particular TiO$_2$ memristor, which is often used as a reference in simulation studies because little data is available on the real HP memristor [9], [12].

The corresponding i-v characteristic $i_M(v_g)$ of the tunneling barrier with parameters from [10] is plotted in Fig. 2 (a) for three different values of w. The curves obviously exhibit negative differential resistance and global activity even for $\Delta w > 0$, which is presented in [11] as the limit of model validity. This behavior does not correspond to the expected characteristics of MIM junctions.
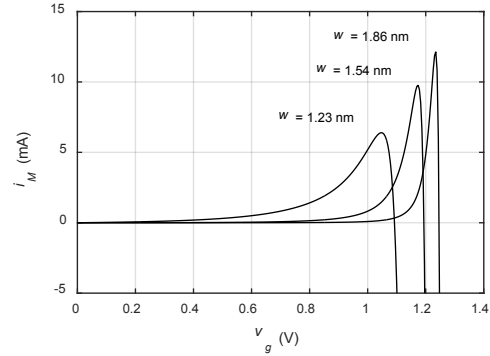

Fig. 2. Static I-V characteristics of the tunnel barrier (3)–(7) for parameters from [10].

The abrupt nonlinearity of $i_M(v_g)$ introduces ambiguity into the solution of the Port Equation (for a given i_M there are two possible values of v_g). This causes non-convergence, numerical errors, and non-physical results during time-domain simulations.

Our paper [14] identifies the root of the problem in the incorrect use of (5a) and (5b), which are only valid for $ev_g \leq \phi_0$ [13], i.e. for $v_g < 0.95$ V for the particular model from [10]. Modifying (5a) and (5b) using the original form from [13] does not solve the problem as the correction introduces a discontinuity to the model. Therefore paper [14] also proposes a behavioral approximation of PE, which matches well the measured characteristics.

The next chapter proposes another solution based on tangential extrapolation.

B. Tangential extrapolation of static I-V characteristics

Fig. 3 shows the static I-V characteristics of Pickett's model [10] in the logarithmic scale. For $v_g > 1$ there is a region of super-exponential growth of current followed by a negative resistance region, which is the result of using (5a) and (5b) outside their domain.

The purpose of the extrapolation is to extend the super-exponential region by the tangent in the logarithmic scale, i.e. by the exponential function.
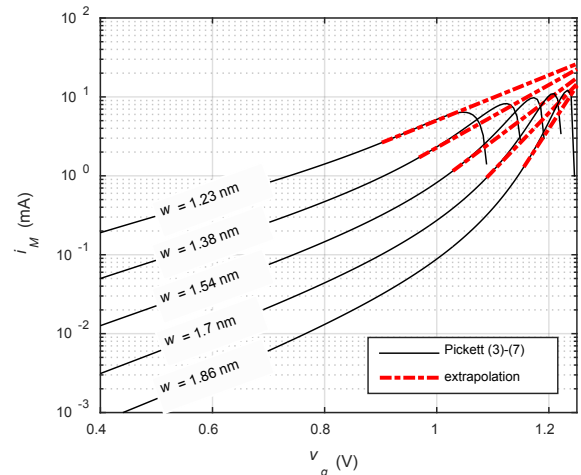

Fig. 3. Extrapolation of the I-V characteristics.

Let us denote $\widetilde{i}_M(v_g)$ the original static characteristic (3)-(7). The proposed modification of PE will be

$$i_M(v_g) = \begin{cases} \widetilde{i}_M(v_g) & \text{for } |v_g| \leq v_{g0}, \\ \widetilde{i}_M(v_{g0})\exp\left[k\left(|v_g| - v_{g0}\right)\right] & \text{for } |v_g| > v_{g0} \end{cases} \quad (9)$$

where

$$k = \left.\frac{d\ln(\widetilde{i}_M)}{dv_g}\right|_{v_g = v_{g0}} = \left.\frac{1}{\widetilde{i}_M(v_{g0})}\frac{d\widetilde{i}_M}{dv_g}\right|_{v_g = v_{g0}}. \quad (10)$$

The proposed extrapolation (9) provides continuity and smoothness at the point v_{g0}. In addition, (9) is monotonous, which leads to the unambiguous memristor static characteristic $i_M(v_M)$. Note that the current levels of the extrapolated region in Fig. 3 may lie above the damage threshold of the device, but the unambiguousness is necessary for correct operation of the Newton iteration algorithm used in the time-domain simulation [15]. During the solution of a system of nonlinear equations the Newton algorithm may call the model with relatively high values of v_g.

Fitting the original characteristics can be improved by the linear dependence of threshold voltage v_{g0} on the barrier width

$$v_{g0} = \alpha + \beta w. \quad (11)$$

The result for $\alpha = 0.9$ and $\beta = 0.36$ is shown in Fig. 3.

The derivative (10) should be expressed analytically for the implementation in the PSpice model. In the exponential region the first term in braces in (3) dominates the expression and the other term can be neglected. Applying standard rules, we obtain an approximation of the first derivative of i_M for $v_g > 0$

$$\frac{di_M}{dv_g} = \frac{-2j}{\Delta w^3}\phi_I\exp\left(-B\Delta w\sqrt{\phi_I}\right)\frac{dw_2}{dv_g} + $$
$$+ \frac{j}{\Delta w^2}\left\{\exp\left(-B\Delta w\sqrt{\phi_I}\right)\left[\frac{d\phi_I}{dv_g} - B\phi_I\left(\frac{dw_2}{dv_g}\sqrt{\phi_I} + \frac{\Delta w}{2\sqrt{\phi_I}}\frac{d\phi_I}{dv_g}\right)\right]\right\}, \quad (12)$$

where

$$\frac{d\phi_I}{dv_g} = -e\frac{w_1 + w_2}{2w} - e|v_g|\frac{1}{2w}\frac{dw_2}{dv_g} + $$
$$+ \frac{1.15\lambda w}{\Delta w}\left(\frac{1}{\Delta w}\ln\left[\frac{w_2(w - w_1)}{w_1(w - w_2)}\right] - \frac{w}{w_2(w - w_2)}\right)\frac{dw_2}{dv_g} \quad (13)$$

and

$$\frac{dw_2}{dv_g} = -2w\frac{9.2\lambda}{\left(3\phi_0 + 4\lambda - 2e|v_g|\right)^2}e. \quad (14)$$

The full listing of the PSpice model is shown in the Appendix.

III. NUMERICAL RESULTS

Fig. 4 compares the static I-V characteristics of the enhanced model with the original Pickett's model [10] for different values of w. The curves were obtained using the DC analysis in PSpice with the voltage source connected across the integrating capacitor C1, which enforces a constant w (see the model listing in Appendix). Up to the threshold v_{g0} the curves are identical. The relative error in the superexponential region lies below 2%.
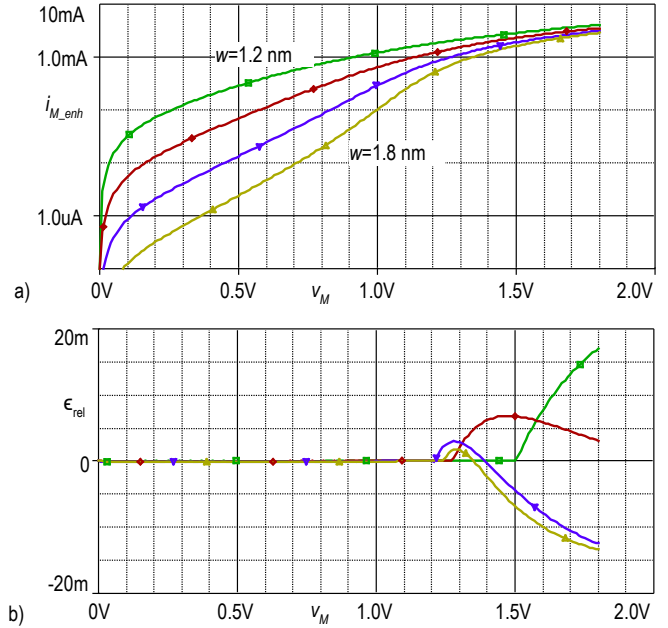

Fig. 4. PSpice simulation of static I-V characteristics of the enhanced model (a); relative error between enhanced and original models (b).

The state equation of the enhanced model has not been changed. Therefore the dynamic behavior of both models is expected to be the same.
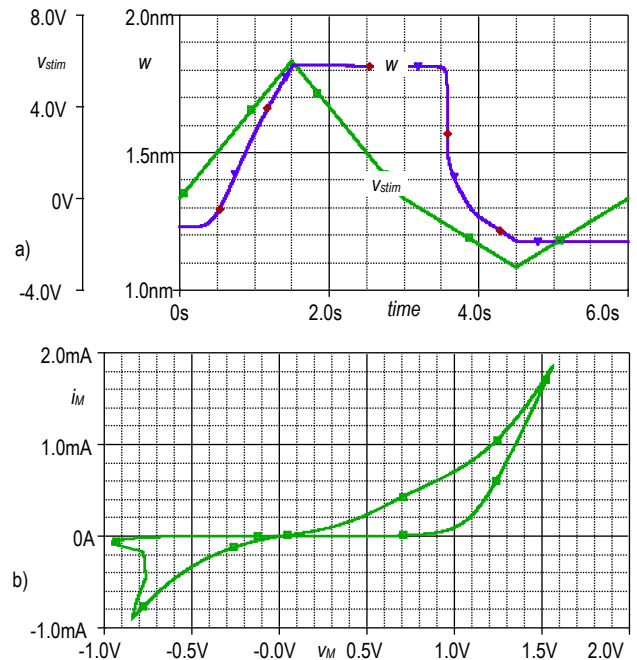

Fig. 5. Time-domain simulation of memristor in series with a 2.4kΩ resistor: driving voltage and barrier width w (a); pinched hysteresis loop (b).

Fig. 5 shows the results of PSpice time-domain simulation of the memristor in connection with a 2.4kΩ resistor driven by a triangular voltage waveform, which is used as a reference circuit [10]. The initial state was $w = 1.228$ nm. The waveforms of $w(t)$ in Fig. 5 a) of the original and the enhanced model are identical, and the pinched hysteresis loop in Fig. 5 b) matches the original model.

The simulation of the static characteristics similar to Fig. 4 but for negative voltage (i.e. from -1.8V to 0V) was not possible due to the non-convergence of the original model.

IV. CONCLUSION

The present modification of Pickett's model eliminates the negative-resistance region from the static I-V characteristics, which makes the solution of the Port Equation unambiguous.

APPENDIX

The PSpice model is a modification of the original Pickett's macromodel from [10]:

```
.SUBCKT tio2mem plus minus PARAMS:
 +phio=0.95 Lm=0.0998 w1=0.1261 foff=3.5e-6
 +ioff=115e-6 aoff=1.2 fon=40e-6 ion=8.9e-6
 +aon=1.8 b=500e-6 wc=107e-3 IC = 1.2

;local parameters
.param Bh = 10.24634
.param explim = 50

;series resistor Rs and its current
Rs int minus 215
EabsiM  absiM  0 value={abs(V(int,minus))/215}

;State Equation: v(w) = barrier width in nm
C1 w 0 1e-9 IC={IC}
R  w 0 1e8MEG
Goff 0 w value={stp(V(int,minus)) *
foff*sinh2(V(absiM)/ioff)*exp2(-exp2(V(mon1))-
V(w)/wc)}
Gon  w 0 value={stp(-V(int,minus))* fon
*sinh2(V(absiM)/ion) *exp2(-exp2(V(mon2))-V(w)/wc)}
Emon1 mon1 0 value={(V(w)-aoff)/wc -(V(absiM)/b)}
Emon2 mon2 0 value={(aon-V(w))/wc  -(V(absiM)/b)}

;Port Equation
Evg avg 0 value={min(abs(V(plus,int)),vg0(v(w)))}
EiM iMlim 0 value={(1/V(dw)**2)
*0.0617*(V(phiI)*exp2(-Bh*v(dw)*V(sr))
+ -(V(phiI)+V(avg))*exp2(-Bh*v(dw)*V(sr2)))}
Emult mult 0 value={if(abs(V(plus,int))>vg0(v(w)),
exp2(v(didvg)/v(iMlim) *(abs(V(plus,int))-
vg0(v(w)))), 1)}
G1 plus int
value={v(mult)*v(iMlim)*sgn(V(plus,int))}

;auxiliary functions
Esr  sr  0 value={sqrt(V(phiI))}
Esr2 sr2 0 value={sqrt(V(phiI)+V(avg))}

EphiI phiI 0 value={phio-
v(avg)*((w1+V(w2))/(2*V(w)))-
1.15*V(Lmda)*V(w)*log(V(R))/V(dw)}
EdphiI dphi 0 value={-((w1+v(w2))/(2*v(w))) -
v(avg)/(2*v(w))*v(dw2dvg)
+ + (0.1148/v(dw)**2) * v(dw2dvg) * log(v(R))
+ - (0.1148/v(dw)) * v(dw2dvg) * v(w)/(v(w2)*(v(w)-
v(w2))))}
```

```
Edi didvg 0 value={-
2*0.0617/(v(dw)**3)*v(dw2dvg)*v(phiI)*exp2(-
Bh*v(dw)*v(sr))
+ +0.0617/(v(dw)**2)  * exp2(-Bh*v(dw)*v(sr))
+ *(v(dphi) - Bh*v(phiI)*(
v(dw2dvg)*v(sr)+0.5*v(dw)/v(sr)*v(dphi)))}

Elamda Lmda 0 value={Lm/V(w)}
Ew2 w2 0 value={w1+V(w)-(0.9183/(2.85+4*V(Lmda)-
2*v(avg)))}
Edw2 dw2dvg 0 value={-2*0.9183/(2.85+4*V(Lmda)-
2*v(avg))**2}
EDw dw 0 value={V(w2)-w1}
ER R 0 value={(V(w2)/w1)*(V(w)-w1)/(V(w)-V(w2))}
.func vg0(w) = {0.9 + 0.36*(w-1.228)}
.func exp2(x) = {if(x>explim,exp(explim)*(1+x-
explim),exp(x))}
.func sinh2(x)= {0.5*(exp2(x)-exp2(-x))}
.ENDS tio2mem
```

REFERENCES

[1] J.J. Yang, D.B. Strukov, D.R. Stewart, "Memristive devices for computing," *Nature Nanotechnology*, 2013, vol. 8, pp. 13–24.
[2] A. Adamatzky, L.O. Chua (eds.), Memristor Networks, New York (USA): Springer, 2014.
[3] D.B. Strukov, G.S. Snider, D.R. Stewart, R.S. Williams, "The missing memristor found," *Nature*, 2008, vol. 453, pp. 80–83.
[4] M. Di Ventra, Y.V. Pershin, L.O. Chua, "Circuit elements with memory: Memristors, memcapacitors, and meminductors," *Proceedings of the IEEE*, 2009, vol. 97, no. 10, pp. 1717–1724.
[5] D. Biolek, Z. Biolek, V. Biolková, "SPICE Modeling of Memristive, Memcapacitative and Meminductive Systems," in *Proc. of the European Conference on Circuit Theory and Design (ECCTD '09)*, Antalya (Turkey), 2009, pp. 249-252.
[6] Y.N. Joglekar, S.J. Wolf, "The elusive memristor: properties of basic electrical circuits," *European Journal of Physics*, 2009, vol. 30, no. 4, pp. 661-675.
[7] Z. Biolek, D. Biolek, V. Biolková, "SPICE model of memristor with nonlinear dopant drift," *Radioengineering*, 2009, vol. 18, no. 2, pp. 210–214.
[8] T. Prodromakis, B.P. Peh, C. Papavassiliou, C. Toumazou, "A versatile memristor model with nonlinear dopant kinetics," *IEEE Transactions on Electron Devices*, 2011, vol. 58, no. 9, pp. 3099–3105.
[9] E. Linn, A. Siemon, R. Waser, S. Menzel, "Applicability of Well-Established Memristive Models for Simulations of Resistive Switching Devices," *IEEE Transactions on Circuits and Systems I: Regular Papers*, 2014, vol.61, no.8, pp. 2402-2410.
[10] M.D. Pickett, D.B. Strukov, J.L. Borghetti, J.J. Yang, G.S. Snider, D.R. Stewart, R.S. Williams, "Switching dynamics in titanium dioxide memristive devices," *Journal of Applied Physics*, 2009, vol. 106, pp. 074508.
[11] H. Abdalla M.D. Pickett, "SPICE modeling of memristors," in *Proc. IEEE Int. Symp. Circuits and Systems*, Rio de Janeiro (Brazil), 2011, pp. 1832–1835.
[12] A. Ascoli, F. Corinto, V. Senger, R. Tetzlaff, "Memristor model comparison," *IEEE Circuits Syst. Mag.*, 2013, vol. 13, no. 2, pp. 89–105.
[13] J. Simmons, "Electric tunnel effect between dissimilar electrodes separated by a thin insulating film," *Journal of Applied Physics*, 1963, vol. 34, no. 9, pp. 2581–2590.
[14] Z. Kolka, D. Biolek, V. Biolkova, "Improved Model of TiO2 Memristor," *Radioengineering*, 2015 (to appear).
[15] J. Vlach, K. Singhal, Computer Methods for Circuit Analysis and Design, 2nd edition, New York (USA): Springer, 1993.